Characterization of High-Spin and Low-Spin Iron(III) Quinoxalinotetraphenylporphyrin

Jacek Wojaczyński, Lechosław Latos-Grażyński,* and Tadeusz Głowiak

Department of Chemistry, University of Wrocław, 14 F. Joliot-Curie Street, Wrocław 50 383, Poland

Received March 14, 1997[⊗]

The ^{1}H NMR spectra of iron(III) quinoxalinotetraphenylporphyrin ((QTPP)Fe^{III}X$_n$), iron(III) (methylquinoxalino)-tetraphenylporphyrin ((MQTPP)Fe^{III}X$_n$), and iron(III) pyrazinotetraphenylporphyrin ((PTPP)Fe^{III}X$_n$) have been studied to elucidate the impact of an aromatic extension of a single pyrrole ring on the electronic structure of the corresponding high- and low-spin iron(III) porphyrins. The ^{1}H NMR spectra of the complexes with the following axial ligands have been reported: chloride, iodide, cyanide, pyridine-d_5 (py-d_5), 4-aminopyridine (4-NH$_2$py), and imidazole (ImH). Modification of the tetraphenylporphyrin by addition of the quinoxaline (pyrazine) fragment results in stabilization of the rare low-spin iron(III) $(d_{xz}d_{yz})^4(d_{xy})^1$ electronic ground state in the presence of axial cyanide or pyridine ligands. The more common $(d_{xy})^2(d_{xz}d_{yz})^3$ electronic ground state has been established for [(QTPP)Fe^{III}(4-NH$_2$py)$_2$]$^+$ and [(QTPP)Fe^{III}(ImH)$_2$]$^+$ species. To account for the substituent contribution, the Hückel linear combination of atomic orbitals (LCAO) method has been used to determine the molecular orbitals involved in the spin density delocalization. The deviation from Curie law observed for [(QTPP)Fe^{III}(CN)$_2$]$^-$ suggests Boltzmann equilibrium $\{(d_{xz})^2(d_{yz})^2(d_{xy})^2(\Psi_{-1})^1 \leftrightarrow (d_{xz})^2(d_{yz})^2(d_{xy})^1(\Psi_{-1})^2\} \rightleftharpoons (d_{xz})^1(d_{yz})^2(d_{xy})^2(\Psi_{-1})^2 \rightleftharpoons (d_{xz})^2(d_{yz})^1(d_{xy})^2(\Psi_{-1})^2$ where Ψ_{-1} is related to the a_{2u} orbital of a regular porphyrin. For the first time in the group of low-spin iron(III) tetraarylporphyrins, the sign reversal of the isotropic shift was directly observed for pyrrole-proton resonances. The structure of (QTPP)Fe^{III}Cl was determined by X-ray crystallography. (QTPP)-Fe^{III}Cl crystallizes in the monoclinic space group $P2_1/c$ with $a = 18.016(5)$ Å, $b = 11.399(3)$ Å, $c = 21.996(5)$ Å, $\beta = 112.22(5)°$, and $Z = 4$. The refinement of 548 parameters and 2696 reflections yields $R_1 = 0.0654$, $R_{w2} = 0.1717$. The (QTPP)Fe^{III}Cl presents features of the high-spin five-coordinate iron(III) tetraphenylporphyrin. The quinoxalinotetraphenylporphyrin macrocycle assumes a saddle-shape geometry.

Introduction

The electronic ground state of low-spin iron(III) porphyrins evolves between two extreme cases, i.e. $(d_{xy})^2(d_{xz}d_{yz})^3$ and $(d_{xz}d_{yz})^4(d_{xy})^1$.[1,1−6] A large variety of axial ligands have been probed in order to elucidate the relation between the ligation and the fine details of the heme electronic structure. ^{1}H NMR spectroscopy of paramagnetic hemoproteins and iron porphyrins provides a particularly useful and sensitive tool for determination of the electronic ground states of the iron.[1] In the group of low-spin iron(III) porphyrins, ^{1}H NMR data have been reported for the following type of axial ligands: pyridine derivatives,[3a,7] alkyl isocyanide (R-NC),[3c,4] dimethyl phenylphosphonite (P(OMe)$_2$Ph),[5] alkyl (R),[8] aryl (Ar),[9] trialkylphosphine (PR$_3$),[10] imidazoles,[6,11] cyanide (CN$^-$),[6,12,13] ammonia,[14] [Si(CH$_3$)$_3$]$^-$, [15] and azaferrocene (η^5-C$_4$H$_4$N)(η^5-C$_5$H$_5$)Fe.[16] Usually the low-spin state is characteristic of bis-ligated species PFe^{III}L$_2$, although some ligands (e.g. alkyls or aryls) generate this state in mono-ligated complexes, PFe^{III}R or PFe^{III}Ar.[7,9]

In the iron(III) tetraarylporphyrin series the rare $(d_{xz}d_{yz})^4(d_{xy})^1$ electronic ground state has been stabilized by ligands which are simultaneously weak σ-donors and strong π-acceptors, such as *t*-BuNC, (4-CN)py, and P(OMe)$_2$Ph.[3−5] On the basis of EPR studies, the analogous electronic ground state was assigned to low-spin iron(III) chlorins for any low-spin type ligand.[3b,17] Recently, it has been demonstrated that selected tetraalkylporphyrins, including chiroporphyrin, also stabilize this uncommon electronic structure of iron(III).[6]

Previously we have investigated the impact of mono-β-substitution of high-spin, (2-X-TPP)Fe^{III}Cl, and low-spin, [(2-X-TPP)Fe^{III}(CN)$_2$]$^-$, iron(III) tetraphenylporphyrins on their ^{1}H NMR features.[18] The seven pyrrole protons provided a direct probe of the spin density around the porphyrin macrocycle. The

* Author to whom correspondence should be addressed.

⊗ Abstract published in *Advance ACS Abstracts,* December 15, 1997.

(1) (a) Walker, F. A.; Simonis, U. In *Biological Magnetic Resonance: NMR of Paramagnetic Molecules*; Berliner, L. J., Reuben, J., Eds.; Plenum Press: New York, 1993; Vol. 12, p 133. (b) La Mar, G. N.; Walker, F. A. In *The Porphyrins*; Dolphin, D., Ed.; Academic Press: New York, 1979; pp 61−312.
(2) (a) Dugad, L. B.; Medhi, O. K.; Mitra, S. *Inorg. Chem*. **1987**, *26*, 1741. (b) Scheidt, W. R.; Geiger, D. K.; Lee, Y. J.; Reed, C. A.; Lang, G. *Inorg. Chem*, **1987**, *26*, 1039.
(3) (a) Safo, M. K.; Walker, F. A.; Raitsimring, A. M.; Walters, W. P.; Dolata, D. P.; Debrunner, P. G.; Scheidt, W. R. *J. Am. Chem. Soc.* **1994**, *116*, 7760. (b) Cheesman, M. R.; Walker, F. A. *J. Am. Chem. Soc.* **1996**, *118*, 7373. (c) Walker, F. A.; Nasri, H.; Turowska-Tyrk, I.; Mohanrao, K.; Watson, C. T.; Shokhirev, N. V.; Debrunner, P. G.; Scheidt, W. R. *J. Am. Chem. Soc.* **1996**, *118*, 12109.
(4) Simonneaux, G.; Hindre, F.; Le Plouzennec, M. *Inorg. Chem.* **1989**, *28*, 823.
(5) Guillemot, M.; Simonneaux, G. *J. Chem. Soc., Chem. Commun.* **1995**, 2093.
(6) (a) Nakamura, M.; Ikeue, T.; Neya, S.; Funasaki, N.; Nakamura, N. *Inorg. Chem.* **1996**, *35*, 3731. (b) Nakamura, M.; Ikeue, T.; Fujii, H.; Yoshimura, T. *J. Am. Chem. Soc*. **1997**, *119*, 6284. (c) Wołowiec, S.; Latos-Grażyński, L.; Mazzanti, M.; Marchon, J.-P. *Inorg. Chem.* **1997**, *36*, 5761.
(7) La Mar, G. N.; Bold, T. J.; Satterlee, J. D. *Biochim. Biophys. Acta* **1977**, *498*, 189.
(8) Balch, A. L.; Hart, R. H.; Latos-Grażyński, L.; Traylor, T. G. *J. Am. Chem. Soc*. **1990**, *112*, 7382.
(9) Balch, A. L.; Renner, M. W. *Inorg. Chem.* **1986**, *25*, 303.
(10) Simonneaux, G.; Sodano, P. *Inorg. Chem.* **1988**, *27*, 3956.
(11) Satterlee, J. D.; La Mar, G. N. *J. Am. Chem. Soc.* **1976,** *98*, 2804.
(12) La Mar, G. N.; Del Gaudio, J.; Frye, J. S. *Biochim. Biophys. Acta* **1977**, *498*, 422.
(13) Wołowiec, S.; Latos-Grażyński, L. *Inorg. Chem*. **1994**, *33*, 3576.
(14) Kim, Y. O.; Goff, H. M. *Inorg. Chem.* **1990**, *29*, 3907.
(15) Kim, Y. O.; Goff, H. M. *J. Am. Chem. Soc*. **1988**, *110*, 8706.
(16) Wołowiec, S.; Latos-Grażyński, L.; Zakrzewski, J. *New J. Chem*. **1996,** *20*, 939.
(17) (a) Stolzenberg, A. M.; Strauss, S. H.; Holm, R. H. *J. Am. Chem. Soc.* **1981**, *103*, 4763. (b) Coulter, E. D.; Sono, M.; Chang, C. K.; Lopez, O.; Dawson, J. H. *Inorg. Chim. Acta* **1995**, *240*, 603.
(18) Wojaczyński, J.; Latos-Grażyński, L.; Hrycyk, W.; Pacholska, E.; Rachlewicz, K.; Szterenberg, L. *Inorg. Chem.* **1996**, *35*, 6861.

S0020-1669(97)00305-4 CCC: $14.00

Scheme 1

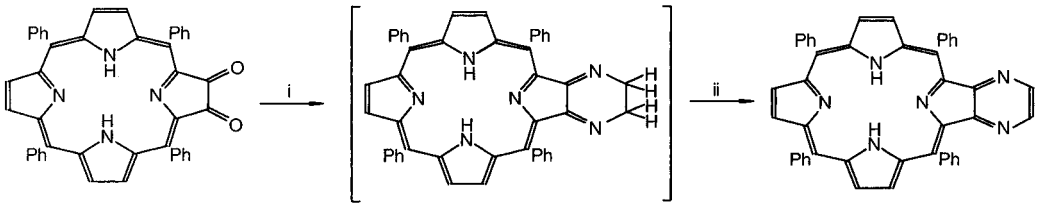

domination of the $(d_{xy})^2(d_{xz}d_{yz})^3$ electronic ground state, which is typical for $[(TPP)Fe^{III}(CN)_2]^-$, has been observed in the ^1H NMR investigations of these monopyrrole-substituted iron(III) tetraphenylporphyrins.

Here we describe further studies on the controlled modification of the tetraarylporphyrin periphery by a selective symmetrical extension of a single pyrrole ring. We have considered the possibility that the appropriate substitution of the equatorial porphyrin may be sufficient to modify the coordination environment of iron(III), forcing the preference of the $(d_{xz}d_{yz})^4(d_{xy})^1$ electronic ground state. We have focused on iron(III) complexes of quinoxalinoporphyrin ($QTPPH_2$) and related ligands.

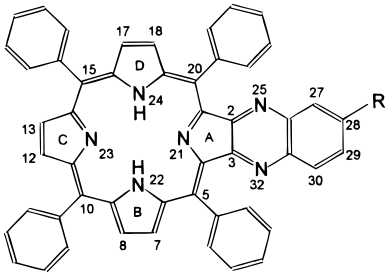

The synthetic procedure for this porphyrin was elaborated by Crossley *et al.* in their investigations of rigid laterally-bridged oligoporphyrins.[19−24] It was shown that a disubstitution of the free base porphyrin originates a substantial bond fixation in the macrocyclic system but not for the corresponding palladium(II) or copper(II) complexes.[19] Thus, quinoxalinoporphyrin has a chlorin-like π-delocalization pathway.[19,22,23] The conjugation pathway analyzed theoretically for oligoporphyrins connected by 1,4,5,8-tetrazaanthracene demonstrates a weak interaction between porphyrin and the aromatic bridge unit contrary to an anticipated aromatic π-delocalization.[22] By analogy it might suggest an efficient isolation of porphyrin and quinoxaline moieties in quinoxalinoporphyrins.

This work is concerned with the physical characterization of high- and low-spin iron(III) complexes of quinoxalinoporphyrin. We have found that the modification of the tetraphenylporphyrin by addition of the quinoxaline fragment results in stabilization of the low-spin iron(III) $(d_{xz}d_{yz})^4(d_{xy})^1$ electronic ground state, even in the presence of axial cyanide or pyridine ligands.

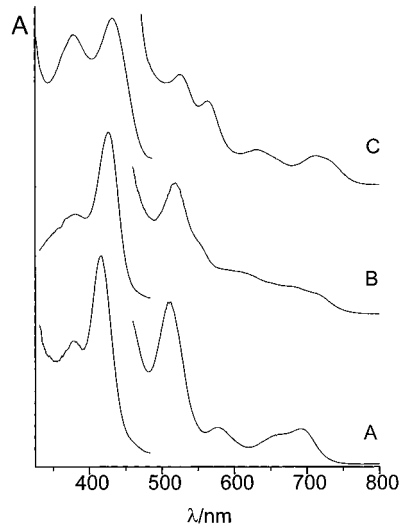

Figure 1. Electronic spectra of $(TPP)Fe^{III}Cl$ (A), $(PTPP)Fe^{III}Cl$ (B), and $(QTPP)Fe^{III}Cl$ (C) in dichloromethane.

Results and Discussion

Synthesis and Characterization of Iron(III) Quinoxalinotetraphenylporphyrin. Quinoxalinotetraphenylporphyrin has been synthesized by benzoyloxation of tetraphenylporphyrin, with hydrolysis to 2-hydroxytetraphenylporphyrin, followed by oxidation with SeO_2 to produce 17,18-dioxo-5,10,15,20-tetraphenylchlorin.[20,25,26] The condensation of 17,18-dioxo-5,10,-15,20-tetraphenylchlorin with 1,2-phenylenediamine or 3,4-diaminotoluene gave quinoxalinotetraphenylporphyrin ($QTPPH_2$)[19] and (methylquinoxalino)tetraphenylporphyrin ($MQTPPH_2$), respectively. The analogous synthetic route, using 1,2-ethylenediamine, results in an addition of a pyrazine ring, yielding pyrazinotetraphenylporphyrin ($PTPPH_2$), as shown in Scheme 1. Disubstituted derivatives of $PTPPH_2$ were recently obtained by Crossley *et al.* by a different method utilizing a "reverse" approach to extended porphyrin systems.[24]

The insertion of iron into $QTPPH_2$, $MQTPPH_2$, or $PTPPH_2$ resulted in the formation of $(QTPP)Fe^{III}Cl$, $(MQTPP)Fe^{III}Cl$, and $(PTPP)Fe^{III}Cl$, respectively. The electronic spectra of $(PTPP)Fe^{III}Cl$ and $(QTPP)Fe^{III}Cl$ (Figure 1) are characteristic for high-spin iron(III) tetraphenylporphyrins.[27] The extension of the aromatic system causes shifts of all bands and changes in their relative intensity as compared to $(TPP)Fe^{III}Cl$. The EPR spectra of $(QTPP)Fe^{III}Cl$ and $(PTPP)Fe^{III}Cl$ demonstrate char-

(19) Crossley, M. J.; Burn, P. L.; Chew, S. S.; Cuttance, F. B.; Newsom, I. A. *J. Chem. Soc., Chem. Commun.* **1991**, 1564.
(20) Crossley, M. J.; Burn, P. L.; Langford, S. J.; Pyke, S. M.; Stark, A. G. *J. Chem. Soc., Chem. Commun.* **1991**, 1567.
(21) Crossley, M. J.; Burn, P. L. *J. Chem. Soc., Chem. Commun.* **1991**, 1569.
(22) Lü, T. X.; Reimers, J. R.; Crossley, M. J.; Hush, N. S. *J. Phys. Chem.* **1994**, *98*, 11878.
(23) Crossley, M. J.; Govenlock, L. J.; Prashar, J. K. *J. Chem. Soc., Chem. Commun.* **1995**, 2379.
(24) Crossley, M. J.; King, L. G.; Newsom, I. A.; Sheehan, C. S. *J. Chem. Soc., Perkin Trans. 1* **1996**, 2675.
(25) Crossley, M. J.; Harding, M. M.; Sternhell, S. *J. Org. Chem.* **1988**, *53*, 1132.
(26) Callot, H. *Bull. Soc. Chim. Fr.* **1974**, 1492.
(27) Małek, A.; Latos-Grażyński, L.; Bartczak, T. J.; Żądło, A. *Inorg. Chem.* **1991**, *30*, 3222.

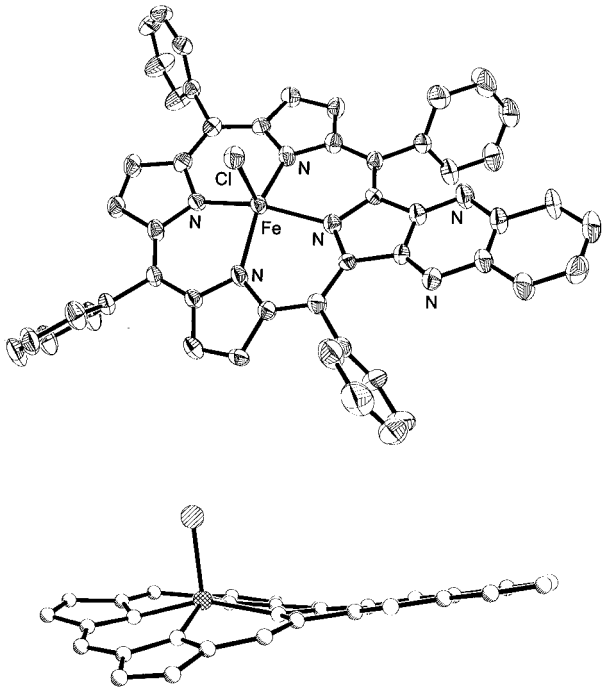

Figure 2. Perspective drawing of (QTPP)$Fe^{III}Cl$ with 30% thermal elipsoids and the projection of the porphyrin core. The phenyl groups are omitted from the side view for clarity.

acteristic features of the $S = {}^5/_2$ electronic state with strong $g_\perp = 6$ and weak $g_\parallel = 2$ signals.[28] The relevant ^{1}H NMR spectra of (QTPP)$Fe^{III}Cl$ and (PTPP)$Fe^{III}Cl$ present a pattern of high-spin ($S = {}^5/_2$) five-coordinate iron(III) porphyrin complexes (Table 1).[1,27]

Crystal Structure of (QTPP)$Fe^{III}Cl$. The structure of (QTPP)$Fe^{III}Cl\cdot 0.5CH_2Cl_2$ has been determined by X-ray crystallography and is shown in Figure 2. Selected interatomic distances and angles are given in Table 2. Iron(III) has an approximate square pyramidal geometry with the chloride ligand lying at the unique apex. The metal−nitrogen distance to the modified pyrrole (2.093(7) Å) is longer than to the remaining three nitrogens: N(22), 2.048(7) Å; N(23), 2.061(6) Å; and N(24), 2.045(7) Å. In (TPP)$Fe^{III}Cl$ the four Fe−N distances are equal (2.049(9) Å).[29] Thus, they are comparable to the Fe−N distances of (QTPP)$Fe^{III}Cl$. Similarly, as observed in high-spin iron(III) hydroporphyrins, the metal-to-pyrroline nitrogen distance is longer than iron-to-pyrrole nitrogen bond lengths: 2.116(6) Å vs 2.040(6) Å.[30] Likewise the Fe^{III}−Cl distance, 2.216(3) Å, is similar to that in (TPP)$Fe^{III}Cl$ (2.192-(12) Å).[29] The iron is displaced 0.515 Å out of the mean porphyrin plane of 24 atoms toward the axial chloride in comparison to 0.38 Å from the mean porphyrin plane in (TPP)-$Fe^{III}Cl$.[29] The quinoxaline ring is almost coplanar with the attached pyrrole ring. The dihedral angle between the quinoxaline ring and this pyrrolic plane equals 4.0°. The macrocyclic core in (QTPP)$Fe^{III}Cl$ is far from being planar. Figure 3 gives out of plane distances for the atoms in the porphyrin core from the mean porphyrin plane. The pyrrole rings are displaced alternately above and below the mean plane of the porphyrin. The conformation of the porphyrin macrocycle can be described as saddle-shaped.

Table 1. ^{1}H NMR Data[a]

	δ (ppm)				
compd	pyrrole-H	*o*-Ph	*m*-Ph	*p*-Ph	subst-H
(PTPP)$Fe^{III}Cl$	81.0 (4H), 76.1 (2H)	~7.5 (4H), ~5.0 (4H)	13.6 (4H), 12.6 (2H), 12.4 (2H)	7.3 (2H), 6.2 (2H)	11.0 (2H)
(QTPP)$Fe^{III}Cl$	81.6 (2H), 80.9 (2H), 74.2 (2H)	~7.5 (4H), ~5.0 (4H)	13.9 (2H), 13.5 (2H), 12.8 (2H), 12.3 (2H)	7.4 (2H), 6.2 (2H)	10.9 (2H, 27,30-H), 8.8 (2H, 28,29-H)
(MQTPP)$Fe^{III}Cl$	80.5 (2H), 79.9 (2H), 73.2 (2H)	~7.5 (4H), ~5.0 (4H)	13.7 (2H), 13.3 (2H), 12.6 (2H), 12.2 (2H)	7.3 (2H), 6.2 (2H)	10.7 and 10.6 (27,30-H), 8.4 (29-H), 4.8 (3H, CH_3)
(QTPP)$Fe^{III}I$	83.0 (2H), 81.5 (2H), 74.7 (2H)	12.8 (2H), 12.0 (2H), 6.7 (4H)	16.2 (2H), 15.8 (2H), 14.4 (2H), 13.9 (2H)	8.8 (2H), 7.6 (2H)	13.0 (2H, 27,30-H), 9.7 (2H, 28,29-H)
(MQTPP)$Fe^{III}I$	84.3 (2H), 82.9, 82.4, 75.6 (2H)	12.4 (2H), 12.0 (2H), ~6.5 (4H)	16.2 (2H), 15.9 (2H), 14.5 (2H), 13.9 (2H)	8.7 (2H), 7.6 (2H)	12.9 and 12.8 (27,30-H), 9.3 (29-H), 6.0 (3H, CH_3)
$[(QTPP)Fe^{III}]_2O$	13.4 (2H), 13.3 (2H), 13.0 (2H)	7.2−8.2	7.2−8.2	7.2−8.2	7.2−8.2
$[(PTPP)Fe^{III}(CN)_2]^-$ [b]	2.1 (2H), 1.1 (2H), 0.6 (2H)	6.0 (4H), 5.6 (4H)	9.9 (4H), 9.8 (4H)	6.7 (2H), 6.5 (2H)	8.7 (2H)
$[(QTPP)Fe^{III}(CN)_2]^-$ [b]	3.5 (2H) and 0.7 (2H), 1.3 (2H)	5.9 (4H), 5.6 (4H)	10.2 (4H), 9.9 (4H)	6.8 (2H), 6.4 (2H)	8.0 (2H, 28,29-H), 7.1 (2H, 27,30-H)
$[(MQTPP)Fe^{III}(CN)_2]^-$ [b]	3.7, 3.6, 1.5, 1.4, 0.8, 0.7	6.0 (2H), 6.0 (2H), 5.7 (2H), 5.7 (2H)	10.1 (4H), 9.9 (2H), 9.9 (2H)	6.8 (2H), 6.4 (2H)	7.9 (29-H), 7.0 and 6.8 (27,30-H), 4.5 (3H, CH_3)
$[(QTPP)Fe^{III}(py)_2]^+$	2.8 (2H), 4.1 (2H), 5.1 (2H)	6.8 (4H), 6.7 (4H)	8.5 (4H), 8.4 (4H)	7.3 (4H), 7.0 (4H)	7.4 (2H), 7.2 (2H)
$[(QTPP)Fe^{III}(ImH)_2]^+$	−12.2 (2H), −15.6 (2H), −21.7 (2H)	5.6 (4H), 5.6 (4H)	7.0 (4H), 6.8 (4H)	6.8 (4H), 6.6 (4H)	5.7 (2H), 5.2 (2H)
$[(QTPP)Fe^{III}(4\text{-}NH_2py)_2]^+$ [c]	−10.2 (2H), −11.4 (2H), −17.5 (2H)	5.8 (4H), 5.6 (4H)	7.5 (4H), 7.4 (4H)	6.9 (4H), 6.7 (4H)	5.9 (2H), 5.2 (2H)

[a] All spectra recorded in chloroform-*d* at 293−295 K. [b] In methanol-d_4. [c] Resonances of coordinated ligand at 4.5 (NH_2), 0.2 (3,5-H), and −15.7 ppm (2,6-H).

(28) Palmer, G. In *The Porphyrins*; Dolphin, D., Ed.; Academic Press: New York, 1979; Vol. 4, pp 313−353.
(29) Hoard, J. L.; Cohen, G. H.; Glick, M. D. *J. Am. Chem. Soc.* **1967**, *89*, 1992.
(30) Barkigia, K. M.; Chang, C. K.; Fajer, J.; Renner, M. W. *J. Am. Chem. Soc.* **1992**, *114*, 1701, and references cited therein.

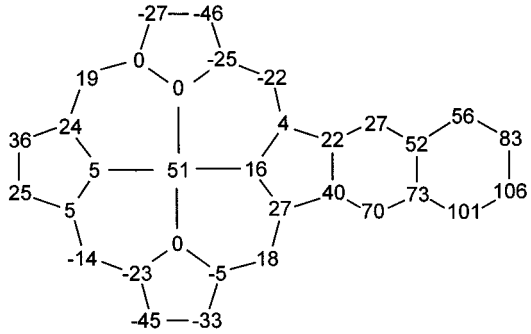

Figure 3. Diagram of the (QTPP)$Fe^{III}Cl$ porphyrinic core. Each atom symbol has been replaced by a number representing the perpendicular displacement (in units of 0.01 Å) from the mean porphyrin plane.

Table 2. Selected Bond Lengths (Å) and Angles (deg) for (QTPP)$Fe^{III}Cl \cdot 0.5CH_2Cl_2$

Fe−Cl	2.216(3)	Fe−N(23)	2.061(6)
Fe−N(21)	2.093(7)	Fe−N(24)	2.045(7)
Fe−N(22)	2.048(7)		
N(21)−Fe−N(22)	87.1(3)	N(23)−Fe−N(24)	87.0(3)
N(21)−Fe−N(23)	157.1(3)	N(21)−Fe−Cl	102.5(2)
N(21)−Fe−N(24)	87.1(3)	N(22)−Fe−Cl	104.2(2)
N(22)−Fe−N(23)	87.5(3)	N(23)−Fe−Cl	100.4(2)
N(22)−Fe−N(24)	150.9(3)	N(24)−Fe−Cl	104.9(2)

Characterization and Spectral Assignments for High-Spin Iron(III) Quinoxalinotetraphenylporphyrin Complexes. The ^1H NMR data have been analyzed in the context of C_s symmetry for high-spin complexes (the symmetry plane passing through N(21), N(23), and Fe atoms) and C_{2v} in the case of low-spin complexes (the main C_2 axis passing through N(21), Fe, and N(23) atoms).

In both cases there are three distinct pyrrole positions, (7, 18), (8, 17), and (12, 13), and two different *meso* positions, (5, 20) and (10, 15). Considering the structural constraints, two para, four ortho, and four meta phenyl resonances may be expected for the five-coordinated high-spin iron complexes since two opposite sides of the porphyrin are not equivalent. On the other hand, two ortho, two meta, and two para phenyl resonances are expected for dicyano low-spin iron(III) quinoxaline-substituted tetraphenylporphyrins (C_{2v}) since the molecule is additionally symmetrical with respect to the porphyrin plane. Representative spectra of high-spin (QTPP)$Fe^{III}I$ and (MQTPP)-$Fe^{III}I$ complexes are shown in Figure 4. Resonance assignments which are given in Figure 4 and in Table 1 have been made on the basis of relative intensities, line widths, and site-specific methylation. Resonances of *meso*-phenyls have been located in the region that is typical for high-spin iron(III) porphyrins.[1,18,27,31,32] The three inequivalent pyrrole positions should produce three downfield shifted pyrrole resonances for well-resolved spectra, which is particularly well-demonstrated in the case of the iodide derivatives. The pyrrole resonances revealed notable sensitivity to substitution of the quinoxaline fragment. The clearly defined splitting of one of the pyrrole resonances in comparison to (QTPP)$Fe^{III}I$ has been observed due to the methylation at the peripheral quinoxaline position.

Spectral Characterization of Low-Spin Iron(III) Quinoxalinotetraphenylporphyrin. Addition of an excess of potassium cyanide to a solution of (QTPP)$Fe^{III}Cl$ in methanol-d_4 results in its conversion to a six-coordinate low-spin complex: $[(QTPP)Fe^{III}(CN)_2]^-$, which is stable with respect to autoreduction.[33] Usually low-spin iron(III) porphyrins, formed by coordination of two cyanide ligands, produce very narrow paramagnetically shifted resonances due to the optimal relaxation properties.[12,34] The representative ^1H NMR spectrum for $[(QTPP)Fe^{III}(CN)_2]^-$ is shown in Figure 5. The chemical shift values are collected in Table 1. The characteristic sets of three pyrrole resonances of $[(QTPP)Fe^{III}(CN)_2]^-$ (or $[(PTPP)Fe^{III}(CN)_2]^-$) and six of its methylated counterparts $[(MQTPP)Fe^{III}(CN)_2]^-$ (Table 1), unusually located in the 0.6−3.6 ppm region (293 K), are of importance in describing the ground state electronic structure. These pyrrole resonances are accompanied by two, for $[(QTPP)Fe^{III}(CN)_2]^-$ (or $[(PTPP)Fe^{III}(CN)_2]^-$), and four, for $[(MQTPP)Fe^{III}(CN)_2]^-$, sets of ortho and para *meso*-phenyl proton resonances which reveal upfield isotropic shifts and corresponding sets of meta resonances with opposite, i.e. downfield, isotropic shifts.

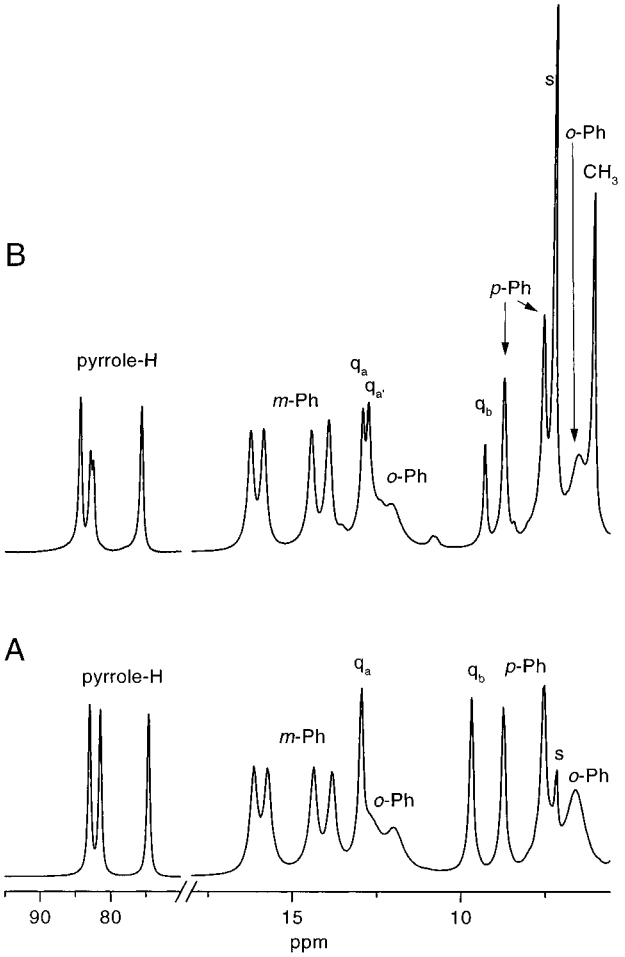

Figure 4. 300 MHz ^1H NMR spectra of (QTPP)$Fe^{III}I$ (A) and (MQTPP)$Fe^{III}I$ (B) in chloroform-*d* solution at 293 K. Resonance assignments: *o*-Ph, *m*-Ph, and *p*-Ph, *o*, *m*, and *p*-phenyl protons, respectively; q, quinoxaline protons (q_a, (q_a'), 27,30-H; q_b, (28),29-H); pyrrole-H, pyrrole protons; *s*, solvent; CH_3, methyl protons. The relative intensity of the +20 to −5 ppm region in traces A and B reduced 3 times relative to the left part of the spectrum.

In our case, the primary assignment could be made on the basis of the chemical shift positions of the resonances, their intensities, and their multiplet structure due to *J*-coupling. A two-dimensional COSY experiment has been shown to be effective in connecting pyrrole proton resonances in iron(III)

(31) Bertini, I.; Luchinat, C. *NMR of Paramagnetic Molecules in Biological Systems*; The Benjamin/Cummings Publishing Co.: Reading, MA, 1986.
(32) Behere, D. V.; Birdy, R.; Mitra, S. *Inorg. Chem.* **1982**, *21*, 386.
(33) La Mar, G. N.; Del Gaudio, J. *Adv. Chem. Ser.* **1977**, *No. 162*, 207.
(34) La Mar, G. N.; Viscio, D. B.; Smith, K. M.; Caughey, W. S.; Smith, M. L. *J. Am. Chem. Soc.* **1978**, *100*, 8085.

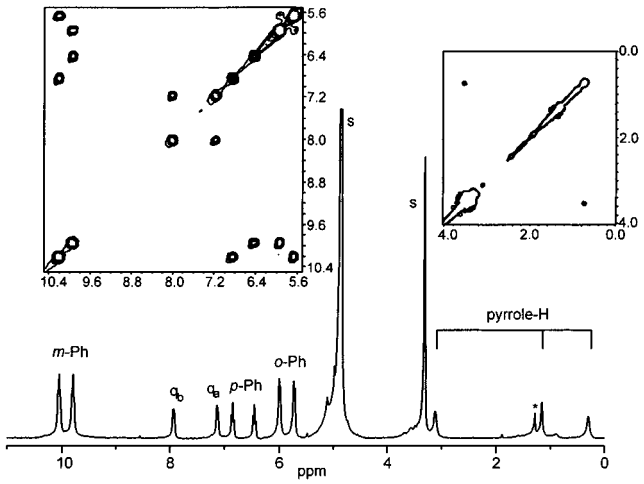

Figure 5. 300 MHz ^{1}H NMR spectrum of $[(QTPP)Fe^{III}(CN)_2]^-$ in methanol-d_4 solution at 300 K. Resonance assignments follow those of Figure 4 (impurities indicated by asterisk). Insets present the 2D COSY ^{1}H NMR maps collected at 293 K.

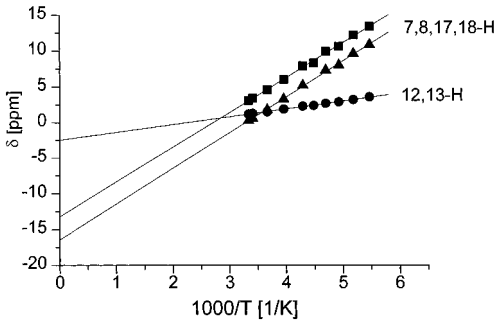

Figure 6. Curie plots of pyrrole resonances of $[(QTPP)Fe^{III}(CN)_2]^-$ in methanol-d_4.

complexes of tetraarylporphyrins.[13,18,35] Two insets in Figure 5 present the COSY maps of $[(QTPP)Fe^{III}(CN)_2]^-$. A cross-peak identifies scalar coupling between protons located on the same pyrrole ring. Similarly we could easily separate phenyl proton signals into two subsets, each assigned to individual *meso*-phenyls. The temperature dependencies of the pyrrole chemical shifts for $[(QTPP)Fe^{III}(CN)_2]^-$ are shown in Figure 6. The shifts vary linearly with T^{-1} but the extrapolated lines do not pass through the positions expected for the diamagnetic references. Thus, the pyrrole shifts do not follow Curie law. The originally *negative* isotropic shifts of the 7, 8, 17, and 18 pyrrole protons at 293 K turn *positive* at 203 K. An anti-Curie behavior of pyrrole resonances was observed previously for bis(isocyanide) and bis(phosphonite) complexes of iron(III) tetraphenylporphyrin, but they did not change signs of isotropic shifts in the observed temperature range.[4,5]

^{1}H NMR spectra of $[(QTPP)Fe^{III}(py\text{-}d_5)_2]^+$, $[(QTPP)Fe^{III}(4\text{-}NH_2py)_2]^+$ and $[(QTPP)Fe^{III}(ImH)_2]^+$ (Figure 7, Table 1) demonstrate the strong dependence of the spectral pattern on the axial ligand. The most basic ligands, i.e. 4-NH_2py and imidazole, produce spectra which resemble those for the analogous species in the tetraphenylporphyrin series. $[(QTPP)Fe^{III}(py\text{-}d_5)_2]^+$ has the pyrrole resonances in the diamagnetic region (5.1, 4.1, and 2.8 ppm; 293 K) contrary to $[(TPP)Fe^{III}(py)_2]^+$ (−11 ppm, 293 K), which demonstrates the typical upfield shift of low-spin iron(III) porphyrins with $(d_{xy})^2(d_{xz}d_{yz})^3$ electronic ground state.[1]

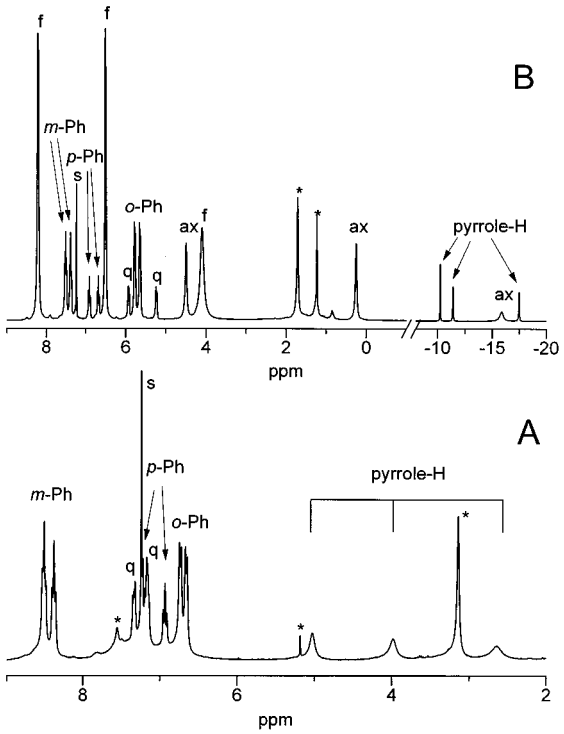

Figure 7. 300 MHz ^{1}H NMR spectra of (A) $[(QTPP)Fe^{III}(py\text{-}d_5)_2]^+$ and (B) $[(QTPP)Fe^{III}(4\text{-}NH_2py)_2]^+$ in $CDCl_3$ solution at 293 K: Resonance assignments: ax, coordinated axial ligand; f, free aminopyridine; the other labels follow those of Figures 4 and 5.

Analysis of π-Delocalization Mechanism in Quinoxalinoporphyrin. Usually the π-delocalization of unpaired spin density in metalloporphyrins is described in terms of ligand-to-metal and metal-to-ligand charge transfer.[1] Spin densities at the particular carbons are related to the pattern of the occupied 3e(π) and unoccupied 4e*(π) molecular orbitals.[1,18,36−38] Here, the Hückel calculations have been carried out for the quinoxalinoporphyrin dianion.[39] The idealized geometry of the dianion has been used. The molecular orbitals of the quinoxalinoporphyrin dianion are related to orbitals of the D_{4h} porphyrin as follows: Ψ_{-3}, $\Psi_{-4} \rightarrow$ 3e(π); $\Psi_{-2} \rightarrow a_{1u}$; $\Psi_{-1} \rightarrow a_{2u}$; Ψ_1, $\Psi_2 \rightarrow$ 4e*(π). They are presented in Figure 8. In general, these molecular orbitals resemble the patterns determined for dihydroporphyrins.[37] The substitution of the pyrrole ring removes the degeneracy of 3e(π) and 4e*(π) orbitals. The lower symmetry opens new routes for the π-density transfer; e.g. the Ψ_{-2} orbital which corresponds to a_{1u} of porphyrin is now symmetry allowed to overlap with d_{xz} and d_{yz} orbitals of iron. In the situation of rhombic splitting, the degeneracy of the iron(III) d_{xz} and d_{yz} orbitals is removed and the spin delocalization is directed to pyrroles A and C (Ψ_{-4}, Ψ_1) or B and D (Ψ_{-3}, Ψ_2), depending on the localization of the unpaired electron. In the extreme cases, the π-spin density approaches zero for one set of pyrrole rings. If the thermal equilibrium $(d_{xy})^2(d_{yz})^2(d_{xz})^1 \rightleftharpoons (d_{xy})^2(d_{xz})^2(d_{yz})^1$ is involved, the predicted spin density distribution will correspond to the averaged pattern of two

(35) (a) Keating, K. A.; de Ropp, J. S.; La Mar, G. N.; Balch, A. L.; Shiau, F.-Y.; Smith, K. M. *Inorg. Chem.* **1991**, *30*, 3258. (b) Lin, Q.; Simonis, U.; Tipton, A. R.; Norvell, C. J.; Walker, F. A. *Inorg. Chem.* **1992**, *31*, 4216.

(36) Shokhirev, N. V.; Walker, F. A. *J. Phys. Chem.* **1995**, *99*, 17795.

(37) (a) Chatfield, M. J.; La Mar, G. N.; Parker, W. O., Jr.; Smith, K. M.; Leung, H.-K.; Morris, I. K. *J. Am. Chem. Soc.* **1988**, *110*, 6352. (b) Liccocia, S.; Chatfield, M. J.; La Mar, G. N.; Smith, K. M.; Mansfield, K. E.; Anderson, R. R. *J. Am. Chem. Soc.* **1989**, *111*, 6087.

(38) (a) Lisowski, J.; Latos-Grażyński, L.; Szterenberg, L. *Inorg. Chem.* **1992**, *31*, 1933. (b) Balch, A. L.; Latos-Grażyński, L.; Noll, B. C.; Olmstead, M. M.; Szterenberg, L.;. Safari, N. *J. Am. Chem. Soc.* **1993**, *115*, 1422. (c) Balch, A. L.; Latos-Grażyński, L.; Noll, B. C.; Szterenberg, L.; Zovinka, E. P. *J. Am. Chem. Soc.* **1993**, *115*, 11846.

(39) Tan, H.; Simonis, U.; Shokhirev, N. V.; Walker, F. A. *J. Am. Chem. Soc.* **1994**, *116*, 5784.

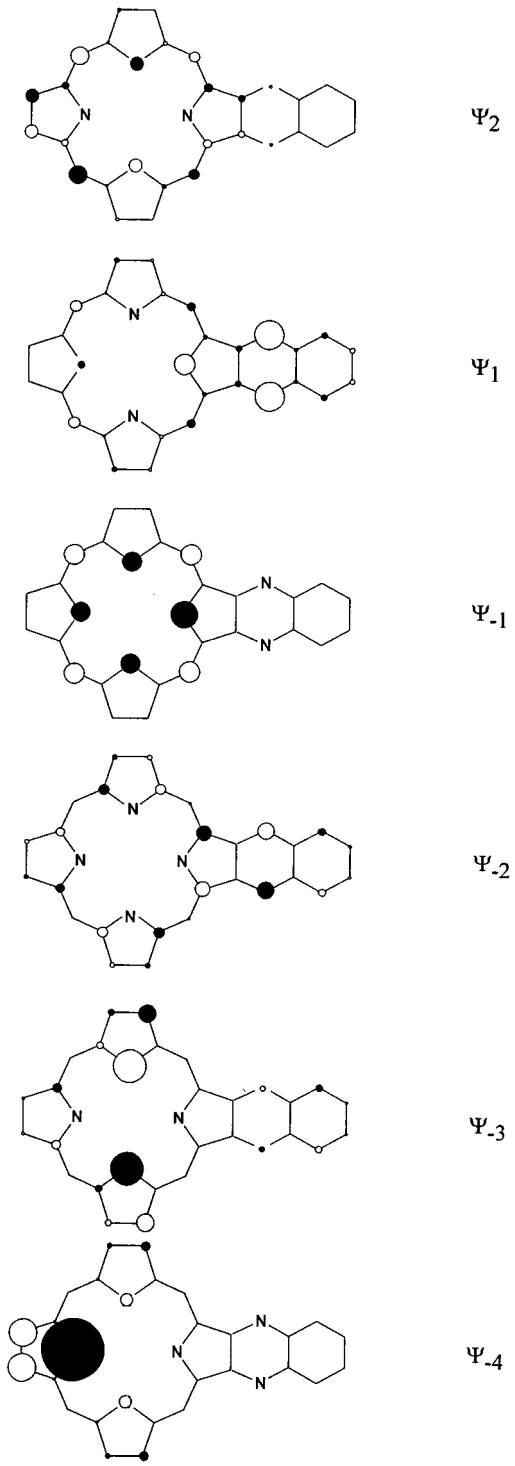

Figure 8. Symmetry properties of the quinoxalinoporphyrin π-orbitals that have proper symmetry and energy to contribute in a delocalization of π-spin density. Phases are indicated by unshaded and filled circles with the size corresponding to unpaired spin density. The orbital numbering is chosen with respect to the HOMO (Ψ_{-1}) according to increasing energy. The following correlation between orbitals of regular porphyrins and substituted porphyrins have been found: $3e(\pi) \rightarrow \Psi_{-3}$, Ψ_{-4}; $a_{1u} \rightarrow \Psi_{-2}$; $a_{2u} \rightarrow \Psi_{-1}$; $4e(\pi)^* \rightarrow \Psi_1$, Ψ_2.

accessible pathways. The relative amount of spin density localized in two directions (AC versus BD) will be temperature dependent, eventually producing a deviation from the Curie dependency of the isotropic shifts. Finally, for the $(d_{xy})^1(d_{yz})^2(d_{xz})^2$ ground electronic state the small contact shift may be predicted unless the admixture of Ψ_{-1} delocalization is accessible to be disclosed by a large concentration of the spin density at *meso* positions (*vide infra*).

The relatively small isotropic shifts of the pyrazine and quinoxaline protons observed for high- and low-spin extended porphyrins (Table 1) allowed the conclusion that orbitals with a large contribution from these fragments are not involved in the extensive delocalization of π-spin densities in any of these electronic states.

Analysis of Isotropic Shift of High-Spin Iron(III) Quinoxalinotetraphenylporphyrin. The electron configuration of the high-spin iron ($S = {}^5/_2$) gives a ^{6}A electronic ground state for which the **g** tensor is isotropic. However, in the case of high-spin iron porphyrins, the zero field splitting (ZFS) generates a dipolar shift proportional to ZFS.[40,41] This dipolar shift contribution at the pyrrole position is notably smaller in the (TPP)Fe^{III}X (X = Cl, Br, I) series than the contact shift contribution and varies in 7−14% of the overall isotropic shift, depending on the axial ligand.[32] The phenyl resonances (meta and para) of (QTPP)Fe^{III}Cl demonstrated an alternation of the isotropic shift although their absolute values are smaller for the para position relative to the meta ones. This is consistent with the contribution of the contact shift combined with the marked addition of the downfield dipolar part.[32,41] We would like to point out that the observed resonances of the (QTPP)Fe^{III}Cl *meso* substituents do not change their position considerably with respect to the (2-X-TPP)Fe^{III}Cl series (Table 1).[18]

At this stage of discussion, we may conclude that the contact shift of high-spin iron(III) quinoxalinotetraphenylporphyrins may result from the simultaneous delocalization in σ as well as both filled Ψ_{-4}, Ψ_{-3} and vacant Ψ_1, Ψ_2 molecular π orbitals. Usually for high-spin iron(III) porphyrins the upfield π-contribution due to delocalization using filled orbitals may be overshadowed by the strong downfield contribution of the σ-mechanism. In our particular case of the quinoxaline derivatives, both π-routes seem to be of importance. Similar analysis has been considered in the case of high-spin β-substituted porphyrins.[18] The spread of the pyrrole resonances, observed for *N*-methyl tetraphenyl high-spin iron(III) porphyrin (*N*-MeTPP)Fe^{III}Cl and high-spin tetraphenyl chlorin (TPC)Fe^{III}Cl (i.e. for two systems with the π-delocalization routes related to (QTPP)Fe^{III}Cl) is probably of the analogous origin.[42,43]

Analysis of Electronic Structure and Isotropic Shift of Low-Spin Iron(III) Quinoxalinotetraphenylporphyrin. The $[(QTPP)Fe^{III}(CN)_2]^-$ spectrum resembles one determined for $[(TPP)Fe^{III}(P(OMe)_2Ph)_2]^+$ or for $[(TPP)Fe^{III}(t\text{-BuNC})_2]^+$ at low temperature limits.[4,5] The observed alternation of the isotropic shift direction of the *meso*-phenyl resonances is characteristic of a π-delocalization mechanism in the phenyl moiety and requires a large amount of π-spin density to be placed at the *meso* carbon. In the case where the dipolar contribution dominates, the phenyl resonances would be shifted in one direction and their shifts would decrease in the order ortho > meta, para.[44] The contribution of the dipolar shift to the isotropic shift increases in the axial ligand series CN^- < py < 4-NH_2py < ImH as estimated by the systematic upfield bias of the meta resonances. Consequently, the quinoxaline resonances shift slightly in the upfield direction, pointing out the small contact contribution at this particular position of the complex.

In the (QTPP)Fe$^{III}X_2$ series we have encountered two examples relevant to two extreme electronic ground states, $(d_{xy})^2(d_{xz}d_{yz})^3$ of $[(QTPP)Fe^{III}(4\text{-}NH_2py)_2]^+$ and $(d_{xz}d_{yz})^4(d_{xy})^1$ of

(40) Kurland, R. J.; McGarvey, B. R. *J. Magn. Reson.* **1970**, *2*, 286.
(41) La Mar, G. N.; Walker, F. A. *J. Am. Chem. Soc.* **1973**, *95*, 6950.
(42) Balch, A. L.; Cornman, C. R.; Latos-Grażyński, L.; Olmstead, M. M. *J. Am. Chem. Soc.* **1990**, *112*, 7552.
(43) Pawlik, M. J.; Miller, P. K.; Sullivan, E. P., Jr.; Levstik, M. A.; Almond, D. A.; Strauss, S. H. *J. Am. Chem. Soc.* **1988**, *110*, 3007.
(44) Goff, H.; La Mar, G. N. *J. Am. Chem. Soc.* **1977**, *99*, 6599.

$[(QTPP)Fe^{III}(CN)_2]^-$. The degeneracy of the $d_{xz}d_{yz}$ orbitals is removed due to the rhombic distortion imposed by the equatorial ligand. The ground state of $[(QTPP)Fe^{III}(py)_2]^+$ corresponds to the situation where the $(d_{xz}d_{yz})^4(d_{xy})^1$ electronic structure is also of importance. We would like to point out that the large participation of the $(d_{xz}d_{yz})^4(d_{xy})^1$ state has been generated here by axial ligands which typically produce the $(d_{xy})^2(d_{xz}d_{yz})^3$ electronic state for iron(III) tetraphenylporphyrin. In the extreme case of $[(QTPP)Fe^{III}(CN)_2]^-$, the sign reversal of the (7,18) and (8,17) pyrrole resonances has been observed, while the 12,13-H resonance preserves the small upfield isotropic shift in the 203−293 K temperature range, but the non-Curie behavior of the isotropic shift with temperature has been also noticed. Consequently, the thermal equilibria will involve the following electronic states $\{(d_{xz})^2(d_{yz})^2(d_{xy})^2(\Psi_{-1})^1 \leftrightarrow (d_{xz})^2(d_{yz})^2(d_{xy})^1(\Psi_{-1})^2\} \rightleftharpoons (d_{xz})^1(d_{yz})^2(d_{xy})^2\ (\Psi_{-1})^2 \rightleftharpoons (d_{xz})^2(d_{yz})^1(d_{xy})^2(\Psi_{-1})^2$ listed in order of the increasing energy. Therefore the spin density pattern of $[(QTPP)Fe^{III}(CN)_2]]^-$ is also consistent with π-delocalization within the Ψ_{-1} (a_{2u}-related) orbital (Figure 8). Evidently, the admixture of the cation radical nature accounts for the contact shift of *meso*-phenyls. The peculiar temperature dependence of the isotropic shift requires practically a two electron occupation of the d_{yz} orbital at the lowest temperature, yielding the positive isotropic shifts at the (7,18) and (8,17) resonances. The admixture of $(d_{xz})^2(d_{yz})^1(d_{xy})^2(\Psi_{-1})^2$ at higher temperature will account for the upfield bias of Curie plots. In principle, the π-spin density may be also transferred to the *meso*-phenyl via the electronic ground state, which includes some $d_{xz}d_{yz}$ character, using Fe → porphyrin π-back-bonding. The unoccupied Ψ_1, Ψ_2 orbitals of quinoxalinoporphyrin, which are symmetry allowed to be involved in the transfer, have large molecular coefficients at the *meso* position, as demonstrated in Figure 8. However, this would imply the large contact shift for the pyrrole positions as well, not seen, however, in the ^1H NMR data.

In other investigated low-spin species, the temperature dependencies of the chemical shifts vary in a typical way. The extrapolated lines of $[(QTPP)Fe^{III}(4\text{-}NH_2py)_2]^+$ do not pass through positions expected for diamagnetic references. The deviations seem to be comparable to those established for $[(TPP)Fe^{III}(ImH)_2]^+$ or $[(\beta\text{-}NO_2TPP)Fe^{III}(ImH)_2]^+$.[27,45] The resonance pattern corresponds to $(d_{xy})^2(d_{yz})^2(d_{xz})^1 \rightleftharpoons (d_{xy})^2(d_{xz})^2(d_{yz})^1$ equilibrium. The $[(QTPP)Fe^{III}(py)_2]^+$ spectrum is representative for the situation of the thermal equilibrium $(d_{xy})^2(d_{xz}d_{yz})^3 \rightleftharpoons (d_{xz}d_{yz})^4(d_{xy})^1$ but under the condition that the $(d_{xy})^2(d_{xz}d_{yz})^3$ state possesses lower energy. In this circumstance, the $[(QTPP)Fe^{III}(py)_2]^+$spectrum at 293 K demonstrates unusually small upfield shifts of the pyrrole resonances (Table 1) which increase when the temperature is lowered.

The analysis of the EPR spectrum of $[(QTPP)Fe^{III}(CN)_2]^-$ in methanol at 77 K offers the description of the electronic ground state consistent with the NMR model. Using Taylor's approach of the "proper" axis definition ($V/\Delta < {}^2/_3$),[28,46] we assign $g_{xx} = -2.51$, $g_{yy} = +2.25$; $g_{zz} = -1.75$, which results in the following tetragonality and rhombocity parameters: $V/\lambda = -2.06$, $\Delta/\lambda = -4.36$, and $V/\Delta = +0.47$. The negative sign of Δ/λ indicates that d_{xy} is higher in energy than either d_{xz} or d_{yz} level (in our case, $d_{xy} > d_{xz} > d_{yz}$). The mixing coefficients in the ground state level $ad_{xz} + bd_{yz} + cd_{xy}$ are as follows: $a = 0.102$, $b = 0.155$, $c = 0.97$, respectively. Thus, the contribution of the d_{xy} orbital to the ground state orbital equals 94.1%. Similar results were obtained for $[(MQTPP)Fe^{III}(CN)_2]^-$ ($g_{xx} = -2.53$, $g_{yy} = +2.26$, $g_{zz} = -1.77$; 95.0% of d_{xy}) and $[(PTPP)Fe^{III}(CN)_2]^-$ ($g_{xx} = -2.46$, $g_{yy} = +2.29$, $g_{zz} = -1.7$; 92% of d_{xy}).

Conclusions

Quinoxalinotetraphenylporphyrin and pyrazinotetraphenylporphyrin seem to be instrumental in stabilization of the $(d_{xz}d_{yz})^4(d_{xy})^1$ electronic ground state in low-spin iron porphyrins. The effect is related to modification of a π-electron system of the porphyrin. Apparently both dianions are better π-acceptors than a tetraphenylporphyrin dianion. This leads to the decrease of energy of the $d_{xz}d_{yz}$ orbitals of iron below the d_{xy} orbital. Analogously to the chlorins,[3,17] the $d_{xz}d_{yz}$ orbitals can be stabilized by $d_{xz}d_{yz}-\pi^*$ interaction, which seems to be more favorable than in the tetraphenylporphyrin case. The chlorin-like π-delocalization pathway has been previously suggested for free quinoxalinotetraphenylporphyrin.[19,22,23] The similar spectroscopic properties of $(QTPP)Fe^{III}$ and $(PTPP)Fe^{III}$ emphasize the fact that a formal extension of pyrazinotetraphenylporphyrin by the phenylene moiety to generate quinoxalinotetraphenylporphyrin has a small influence on the electronic structure of corresponding iron(III) porphyrins.

In conclusion, the appropriate modification of the equatorial porphyrin is sufficient to change the coordination environment of the iron(III) ion, forcing the preference of the $(d_{xz}d_{yz})^4(d_{xy})^1$ electronic state even for axial ligands which are not simultaneously weak σ-donors and strong π-acceptors. The search for other representatives of such iron(III) porphyrins is in progress.

Experimental Section

Methanol-d_4 (Glaser AG) was used as received. Chloroform-*d* ($CDCl_3$ (Glaser AG) was dried before use by being passed through basic alumina.

Quinoxalino[2,3-*b*]tetraphenylporphyrin and methylquinoxalino[2,3-*b*]tetraphenylporphyrin have been synthesized using known procedures.[19,20,25,26]

Pyrazino[2,3-*b*]tetraphenylporphyrin ($PTPPH_2$). A 26 mg (0.04 mmol) sample of 17,18-dioxo-5,10,15,20-tetraphenylchlorin[20,25,26] was dissolved in 30 mL of dichloromethane. A 2 mL aliquot of ethylenediamine was added (the solution immediately became red), and the solution was heated under reflux for 1 h. Silica was added to a cooled reaction mixture. After 24 h, the mixture was subjected to chromatography on silica (Merck; 230−400 mesh; particle size, 0.040−0.063 mm). Elution with dichloromethane−*n*-hexane (40/60 (v/v)) yielded a red fraction which was evaporated to dryness, and the crude porphyrin was recrystallized from CH_2Cl_2−*n*-hexane to give 10 mg of $PTPPH_2$ (37%). ^1H NMR ($CDCl_3$, ppm): 8.89, 8.87 (AB_q, 7,8,17,18-H), 8.71 (s, 12,13-H), 8.56 (s, pyrazine-H), 8.09−8.21 (m, *o*-Ph), 7.70−7.79 (m, *m*,*p*-Ph), −2.78 (bs, NH). UV−vis (CH_2Cl_2; λ_{max}, nm (log ϵ)): 423 (Soret, 5.23), 521 (4.32), 556 (3.87), 592 (3.93), 648 (3.26). HRMS (EI): M/z = 666.254 207 (calcd for $C_{46}N_{30}N_6$, 666.253 195).

Insertion of iron followed a known route to produce (after column chromatography on silica) (μ-oxo)diiron(III) complexes.[47] Corresponding chloro and iodo derivatives were obtained by cleavage of μ-oxo dimeric complexes with the appropriate acid.

Usually, the dicyano-ligated complexes of the investigated iron(III) porphyrin were prepared by dissolution of 2−3 mg of the respective high-spin complex in 0.4 mL of methanol-d_4 saturated with KCN. The titration of 2−3 mg of $(QTPP)Fe^{III}Cl$ in chloroform-*d* with nitrogen bases was applied to generate respective low-spin complexes.

Instrumentation. ^1H NMR spectra were recorded on a Bruker AMX spectrometer operating in the quadrature mode at 300 MHz. The residual ^1H NMR resonances of the deuterated solvents ($CHCl_3$ or CHD_2OD) were used as a secondary reference. The 2D COSY spectrum was collected by use of a typical procedure.[18]

(45) La Mar, G. N.; Walker, F. A. *J. Am. Chem. Soc.* **1973**, *95*, 1782.
(46) Taylor, C. P. S. *Biochim. Biophys. Acta* **1977**, *491*, 137.
(47) Wojaczyński, J.; Latos-Grażyński, L. *Inorg. Chem.* **1995**, *34*, 1044.

Table 3. Crystallographic Data for (QTPP)$Fe^{III}Cl\cdot 0.5CH_2Cl_2$

empirical formula	$C_{50.5}H_{31}N_6FeCl_2$
fw	848.56
cryst syst	monoclinic
space group	$P2_1/c$
unit cell dimens	
a, Å	18.016(5)
b, Å	11.399(3)
c, Å	21.996(5)
α, deg	90
β, deg	112.22(5)
γ, deg	90
V, Å^3	4182(2)
T, K	293(2)
Z	4
cryst size, mm	0.10 × 0.12 × 0.15
d_{calcd}, Mg·m^{-3}	1.348
radiation *λ*, Å	1.541 80 (Cu Kα)
μ(Cu Kα), cm^{-1}	44.08
R indices ($I > 2\sigma(I)$)[a]	
R_1	0.0654
R_{w2}	0.1717

[a] $R_1 = \sum||F_o| - |F_c||/\sum|F_o|$; $R_{w2} = [\sum[w(F_o^2 - F_c^2)^2]/\sum[w(F_o^2)^2]]^{1/2}$.

Absorption spectra were recorded on a diode array Hewlett-Packard 8453 spectrometer. EPR spectra were obtained with a Bruker ESP 300E spectrometer. The magnetic field was calibrated with a proton magnetometer and EPR standards.

Mass spectra were recorded on a ADM-604 spectrometer using the liquid matrix secondary ion mass spectroscopy (8 keV Cs^+ ions) or electron impact techniques.

X-ray Data Collection and Refinement. (QTPP)$Fe^{III}Cl\cdot 0.5CH_2Cl_2$. Crystals of (QTPP)$Fe^{III}Cl\cdot 0.5CH_2Cl_2$ were prepared by diffusion of *n*-hexane into the dichloromethane solution of (QTPP)$Fe^{III}Cl$ contained in a thin tube. Data were collected at 293 K on a Kuma KM-4 diffractometer. The stability of the intensities was monitored by the measurement of three standards every 100 reflections. The data were corrected for Lorentz and polarization effects. No absorption correction was applied. Crystal data are compiled in Table 3.

The structure was solved by the direct methods with SHELXS-86 and refined by the full-matrix least squares method using SHELX-93 with anisotropic thermal parameters for non-H atoms. Scattering factors were those incorporated in SHELXS-93. All the positions of the hydrogen atoms were calculated on the basis of the geometry of the molecule with the isotropic temperature factor fixed at 1.2 times U_{eq} of their parent atoms. The solvent site is occupied by half of a molecule of CH_2Cl_2. A molecule of dichloromethane in the lattice exhibits two disordered positions for the carbon atoms (0.25 occupancy) and four for the chlorine atoms (0.25 occupancy). Distance restraints of C−Cl = 1.77(1) Å and Cl···Cl = 2.89(2) Å were applied for these atoms. All atoms of dichloromethane were refined with their isotropic temperature factors.

Acknowledgment. The financial support of the State Committee for Scientific Research KBN (Grant 3 T09A 143 09) is kindly acknowledged. We would like to thank Professor F. A. Walker and Dr. N. Shokhirev for access to The Molecular Orbital Calculation Package.

Supporting Information Available: Tables listing crystal data, atom coordinates, complete bond lengths and angles, anisotropic displacement coefficients, and calculated hydrogen parameters (8 pages). Ordering information is given on any current masthead page.

IC970305N